Carotenoids: Experimental Ionization Energies and Capacity at Inhibiting Lipid Peroxidation in a Chemical Model of Dietary Oxidative Stress

Pascale Goupy, Michel Carail, Alexandre Giuliani, Denis Duflot, Olivier O. Dangles, Catherine Caris-Veyrat

THE JOURNAL OF PHYSICAL CHEMISTRY B

Article

Cite This: J. Phys. Chem. B 2018, 122, 5860−5869

pubs.acs.org/JPCB

Carotenoids: Experimental Ionization Energies and Capacity at Inhibiting Lipid Peroxidation in a Chemical Model of Dietary Oxidative Stress

Pascale Goupy,[†,‡] Michel Carail,[†,‡] Alexandre Giuliani,[§,∥] Denis Duflot,[⊥] Olivier Dangles,*[,†,‡] and Catherine Caris-Veyrat[†,‡]

[†]INRA, UMR408 SQPOV, 84000 Avignon, France

[‡]Avignon University, UMR408 SQPOV, 84000 Avignon, France

[§]Synchrotron SOLEIL, St-Aubin, BP48, 91192 Gif sur Yvette Cedex, France

[∥]INRA, U1008, BP 71627, 44316 Nantes, France

[⊥]Laboratoire de Physique des Lasers, Atomes et Molécules, UMR CNRS 8523, Université Lille1, 59655 Villeneuve d'Ascq Cedex, France

Supporting Information

ABSTRACT: Carotenoids are important natural pigments and micronutrients contributing to health prevention by several mechanisms, including their electron-donating (antioxidant) activity. In this work, a large series of carotenoids, including 11 carotenes and 14 xanthophylls, have been investigated by wavelength-resolved atmospheric pressure photoionization mass spectrometry (DISCO line of SOLEIL synchrotron), thus allowing the experimental determination of their ionization energy (IE) for the first time. On the other hand, the carotenoids have been also investigated for their ability to inhibit the heme iron-induced peroxidation of linoleic acid in mildly acidic micelles, a simple but relevant chemical model of oxidative stress in the gastric compartment. Thus, the carotenoids can be easily classified from IC_{50} concentrations deduced from the time dependence of the lipid hydroperoxide concentration. With a selection of two carotenes and three xanthophylls a quantitative analysis is also provided to extract stoichio-kinetic parameters. The influence of the carotenoid structure (number of conjugated carbon−carbon double bonds, presence of terminal six-membered rings, hydroxyl, keto, and/or epoxy groups) on the IE, IC_{50}, and stoichio-kinetic parameters is discussed in details. The data show that the antioxidant activity of carotenes is well correlated to their electron-donating capacity, which itself largely depends on the length of the conjugated polyene chain. By contrast, the IE of xanthophylls is poorly correlated to the polyene chain length because of the strong, and sometimes unexpected, electronic effects of the O-atoms. Although IE remains an approximate predictor of the antioxidant activity of xanthophylls, other factors (interaction with the aqueous phase, competing radical-scavenging mechanisms, the residual activity of the antioxidant's oxidation products) probably play a significant role.

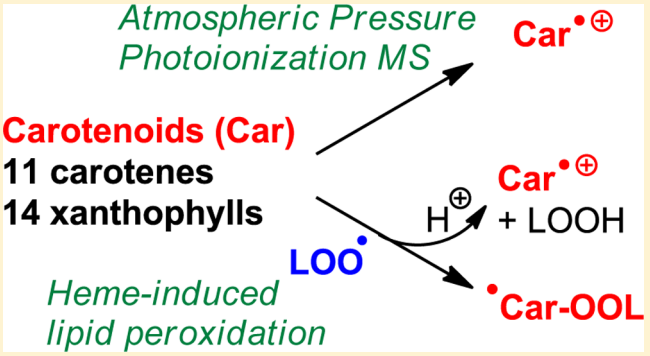

INTRODUCTION

Carotenoids are natural polyenes responsible for the yellow to red colors of many fruits and vegetables.[1] They exhibit a characteristic tetraterpene skeleton of 40 C-atoms involving a chromophore of conjugated double bonds (CDB). Two subclasses can be distinguished: carotenes, which are pure hydrocarbons, and xanthophylls, which are oxygenated and display hydroxyl, oxo, and epoxy groups. Through their bioavailability and bioactivity, carotenoids participate in the nutritional quality of food.[2,3] Carotenes having β-ionone end groups are precursors of vitamin A, xanthophylls accumulating in the macula offer protection against ocular disease,[4] and carotenoids in general help prevent chronic diseases (in particular, cardiovascular disease) due to their capacity for scavenging reactive oxygen species (ROS, antioxidant activity) and their ability to regulate gene expression by interaction with specific receptors.[5]

Carotenoids typically act as antioxidants in multiphasic systems, such as cell membranes and liposomes, food emulsions, and micelles.[6] The antioxidant efficiency varies according to the radical investigated (and thus the method selected), the intrinsic properties of carotenoids and their

Received: April 11, 2018
Revised: May 15, 2018
Published: May 17, 2018

DOI: 10.1021/acs.jpcb.8b03447
J. Phys. Chem. B 2018, 122, 5860−5869

environment.[7,8] Carotenoids can inhibit lipid peroxidation as chain-breaking antioxidants (direct scavenging of the propagating lipid peroxyl radicals). The mechanisms underlining the scavenging of ROS and other free radicals include radical addition and electron transfer, with a possible (minor) contribution of H-atom transfer.[6,9,10] The polyene chain length (number of conjugated double bonds, CDB) is the primary determinant of the radical-scavenging activity. However, cyclization at one or both ends and the presence of functional groups also affect the antioxidant properties of carotenoids.

The first ionization energy (IE) of a molecule is a relevant parameter to assess its intrinsic electron-donating capacity. Being directly related to the energy of the highest occupied molecular orbital (HOMO, IE = $-E_{HOMO}$), IE may be also considered a measure of the nucleophilicity, which could be useful to predict the reactivity with electrophilic oxygen-centered radicals. Several studies have focused on estimating the IE of carotenoids by computational methods, and correlations have been established between the antioxidant capacity and theoretical IE values.[9,11] However, to our knowledge, only one study has addressed the experimental determination of IE for carotenoids (possibly because of the difficulty to place carotenoids in the gas phase). Using photoelectron spectroscopy, the authors obtained for β-carotene: IE = 6.5 eV.[12]

The aim of the present work is to report the experimental determination of the ionization energies for a series of dietary carotenoids, including carotenes and xanthophylls, based on a new mass spectrometry method called wavelength-resolved atmospheric pressure photoionization (APPI) using the radiation DISCO line of SOLEIL synchrotron. The experimental ionization energies will be compared to theoretical values from ab initio Hartree−Fock calculations and related to an experimental IC_{50} parameter expressing the ability of carotenoids to inhibit lipid peroxidation in a simple chemical model of oxidative stress in the gastro-intestinal tract. Finally, with a selection of carotenes and xanthophylls, the lipid peroxidation data will be analyzed quantitatively to extract kinetic and stoichiometric parameters characteristic of the radical-scavenging activity.

EXPERIMENTAL SECTION

Chemicals. Heart metmyoglobin ($MbFe^{III}$, type II, MW ca. 17 600 g mol^{-1}), linoleic acid (LH), and Tween 20 (polyoxyethylenesorbitan monolaurate) were purchased from Sigma-Aldrich (Sigma-Aldrich, Saint-Quentin Fallavier, France). All selected carotenoids were either purchased from CaroteNature (CaroteNature GmbH, Lupsingen, Switzerland) or kindly given by DSM (DSM Nutritional Products Ltd., Kaiseraugst, Switzerland). Other chemicals were purchased from Merck and were of analytical grade. $CHCl_3$ and CH_2Cl_2 were of HPLC grade. All other solvents used were of analytical grade. The phosphate buffers (10 mmol, pH 5.8 or 6.8), prepared with grade water (18 MΩ) purified using a Millipore Q-Plus water purification system (Millipore, MA) were passed through a column of Chelex-100 chelating resin (Bio-Rad, Marnes-la-Coquette, France) to remove contaminating free metal ion traces.

APCI-MS Analysis. 11 carotenes and 15 xanthophylls were dissolved at a concentration of 0.1 g L^{-1} in CH_2Cl_2. All of the experiments were performed with the DISCO beam line at the SOLEIL synchrotron radiation facility (Gif-sur-Yvette, France).[13,14] Photons in the vacuum ultraviolet (VUV) are delivered by a monochromator to the atmospheric pressure experiment branch of the beam lines. This branch is fitted with a differential pumping system that allows delivering windowless VUV photons at the atmospheric pressure.[15] The photon beam crosses at 90° the vapor from a commercial atmospheric pressure photoionization source (Photospray source AB Sciex, Toronto, Canada), in which the discharge lamp has been removed to allow the photons from the beam line instead.[13] The ions are extracted and analyzed by quadrupole time of flight mass spectrometer (QSTAR Pulsar I mass spectrometer, AB Sciex, Toronto, Canada).

The samples were introduced using the flow-injection analysis method: 10 μL of the sample solution at 0.1 g L^{-1} in CH_2Cl_2 was loaded into an injection loop and pushed through the atmospheric pressure photoionization (APPI) source by the solvent (CH_2Cl_2) at a flow rate of 250 μL min^{-1}. The mass spectrometer instrumental parameters were adjusted to obtain the best signal-to-noise ratio and to minimize in-source collision-induced dissociation. Operating parameters: ion source voltage = 1200 V, declustering potential = 20 V, focusing potential = 100 V, and declustering potential = 15 V. The chemical background induced by the solvent was systematically removed by subtracting the mean signal acquired during 1 min before each injection. The photon energy range from 6 to 9 eV was covered by 100 meV steps. The abundance of the radical cation was measured at each photon energy and normalized to the photon flux, as measured by a AXUV 100 photodiode (International Radiation Detector). A linear threshold model was fitted to the experimental data to derive the photoionization threshold (identified with IE) for each molecule.[13]

Inhibition of the Metmyoglobin-Induced Peroxidation of Linoleic Acid. The experimental conditions used were adapted from already published procedures.[16,17] Metmyoglobin ($MbFe^{III}$) was dissolved in 50 mL of a 10 mM phosphate buffer at pH 6.8. Its concentration was standardized at 10 μM using ε = 7700 M^{-1} cm^{-1} at 525 nm. Given volumes of daily prepared solutions of linoleic acid (7 mM), Tween 20 (40 mM), carotenoids (1 mM) in $CHCl_3$ were mixed, and the solvent removed under reduced pressure in darkness and 25 °C. The residue was dissolved immediately in 20 mL of a 10 mM phosphate buffer at pH 5.8 under gentle stirring. Final concentrations: linoleic acid = 0.7 mM, Tween 20 = 2 mM, and carotenoids = 1−5 μM (except lycopene, 1−3 μM because of its poor solubility). Freshly prepared solution (2 mL) was transferred to the spectrometer cells. At time 0, lipid oxidation was initiated by adding 20 μL of the $MbFe^{III}$ solution (final concentration in cell = 100 nM). The UV−visible spectra were recorded at regular time intervals (26 s). Each experiment was repeated 3−4 times at different antioxidant concentrations.

By simply monitoring the accumulation of conjugated dienes (CDs, mainly lipid hydroperoxides, the primary products of lipid oxidation) at 234 nm, an IC_{50} value (antioxidant concentration leading to 50% inhibition) can be estimated. For each antioxidant concentration C, T is defined as the period of time needed to accumulate a given CD concentration. In the absence of antioxidant, T becomes T_0. When $C = IC_{50}$, $T = 2T_0$. Generally, due to a slight curvature in the T vs C plot, a quadratic function is used for the curve fitting: $T/T_0 = 1 + aC + bC^2$. From the optimized a and b parameters, IC_{50} is easily calculated for each antioxidant: $IC_{50} = (\sqrt{(a^2 + 4b)} - a)/2b$.

Alternatively, the time dependence of A (234 nm) can be quantitatively analyzed according to a kinetic model (Scheme

DOI: 10.1021/acs.jpcb.8b03447
J. Phys. Chem. B 2018, 122, 5860−5869

Scheme 1. Kinetic Model for the Metmyoglobin-Induced Peroxidation of Linoleic Acid and its Inhibition by Carotenoids ($MbFe^{III}$: Metmyoglobin, $MbFe^{IV}$: Hypervalent Form, LH: PUFA, LOOH: PUFA Hydroperoxide, and Car: Carotenoid)[a]

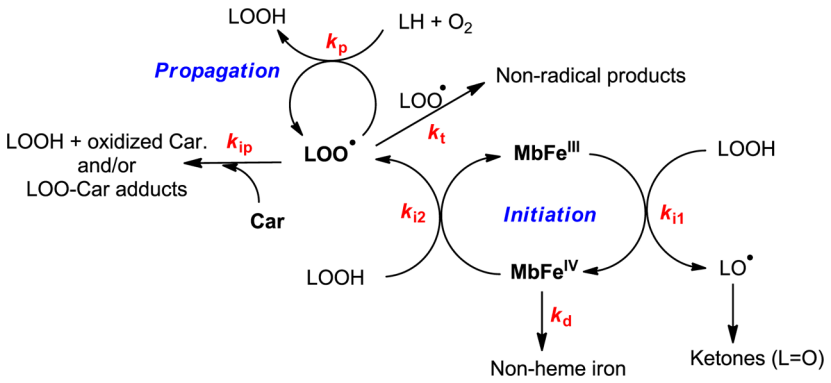

[a]Optimizable parameters for curve fitting analyses are: $r_{ox} = k_p/(2k_t)^{1/2}$, k_{i1}, AE = k_{ip}/k_p, $C_d = k_d/k_{i2}$, and the antioxidant stoichiometry n.

1) developed elsewhere (see Supporting Information).[18] In the absence of antioxidant, the curve fitting yields the polyunsaturated fatty acid (PUFA) oxidizability (r_{ox}) and the rate constant for PUFA hydroperoxide cleavage (k_{i1}). Both parameters are used in the curve fittings of inhibited peroxidation to extract the antioxidant efficiency at inhibiting propagation (AE) and its stoichiometry (n = number of PUFA peroxyl radicals scavenged per antioxidant molecule). All calculations were carried out with the Scientist software (Micromath).

All results are expressed as mean ± standard deviation. Differences in IC_{50} values were calculated using analysis of variance (ANOVA) with Student−Newman−Keuls (SNK) post hoc procedure and considered to be significant at $p < 0.05$.

UV−Visible Spectroscopy. All kinetic experiments were recorded by UV−visible spectroscopy on a Specord diode array spectrometer (Analytik Jena, Germany). Solutions in cells (optical path length: 1 cm) were stirred magnetically and thermostated at 37 (±1) °C.

Calculations. In a first step, semiempirical calculations were carried out by the HyperChem software (Hypercube, Waterloo, Canada) using the PM3 program. Ab initio calculations were then carried out with the Gaussian 09 code. Molecular geometries were optimized at the Restricted Hartree−Fock level using the 6-31G** basis set. For each carotenoid, the vertical ionization energy was obtained from the monoelectronic energy of the highest occupied molecular orbital (HOMO). Indeed, due to error cancellation between relaxation and correlation effects, this energy is known to be close to the experimental value within a few 0.1 eV.[19]

RESULTS

In this work, the carotenoids were selected because of their natural abundance in plant foods or their specific chemical structures. The selection includes (Figures 1 and 2): 5 linear carotenes, 6 mono- or bicyclic carotenes, and 15 xanthophylls with 1−4 oxygenated groups.

Ionization Energy. The ionization energy of series of carotenoids was measured using photon energy-resolved APPI mass spectrometry. An air spray containing the carotenoids is irradiated by the line of a monochromatic radiation and produced photoions if the photon energy is greater than the ionization energy of the compounds. Measuring the abundance of ions according to the photon energy allows determining the ionization threshold of the carotenoids. APPI is an ionization method particularly adapted to nonpolar molecules. Figure 3

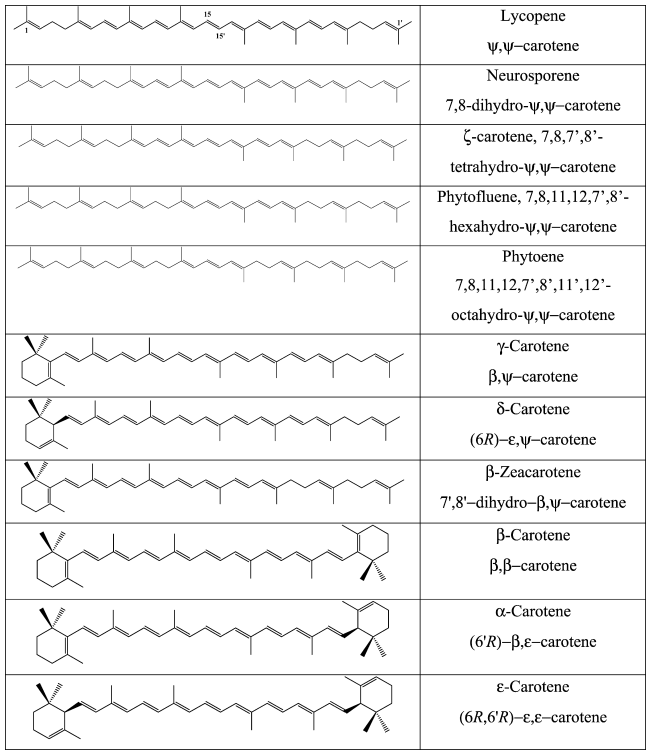

Figure 1. Structure and nomenclature of the carotenes investigated in this work.

shows the abundance (normalized to the photon flux) of the radical cation for lycopene and β-carotene (m/z 536) and for lutein (m/z 569). The photoionization threshold was obtained by fitting a linear threshold function to the data. This procedure was repeated for the other carotenoids with a good reproducibility for both measurement and calculation.

The IE_{exp} values of the carotenoids investigated range from 6.32 to 7.00 eV (Table 1). They were compared to theoretical values (IE_{cal}) obtained with the Gaussian 09 code. For carotenes, IE_{cal} is higher than IE_{exp} with a significant $IE_{exp} - IE_{cal}$ difference from −0.26 to −0.31 eV for linear carotenes and from −0.03 to −0.33 eV for cyclic carotenes. For xanthophylls, the $IE_{exp} - IE_{cal}$ gap is lower and lies between 0.18 and −0.12 eV.

Among linear carotenes, lycopene, which possesses the highest number of CDB in the polyene chain, has the lowest

DOI: 10.1021/acs.jpcb.8b03447
J. Phys. Chem. B 2018, 122, 5860−5869

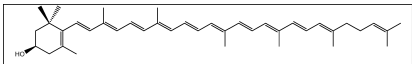	Rubixanthin (3*R*)-β,ψ-caroten-3-ol
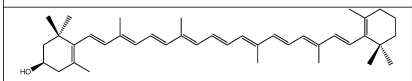	β-Cryptoxanthin (3*R*)-β,β-caroten-3-ol
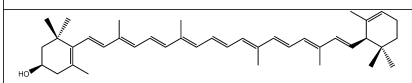	Zeinoxanthin (3*R*,6'*R*)-β,ε-caroten-3-ol
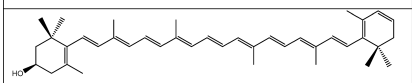	Anhydrolutein III (3*R*)-3',4'-Didehydro-β,β-caroten-3-ol
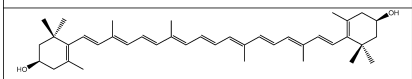	Zeaxanthin (3*R*,3'*R*)-β,β-carotene-3,3'-diol
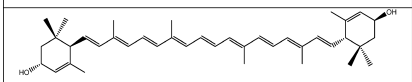	Tunaxanthin E (3*R*,6*R*,3'*S*,6'*S*)-ε,ε-carotene-3,3'-diol
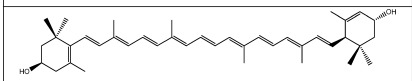	Lutein (3*R*,3'*R*,6'*R*)-β,ε-carotene-3,3'-diol
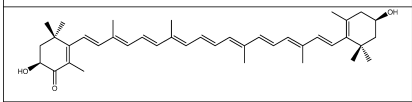	Adonixanthin (3*S*,3'*R*)-3,3'-dihydroxy-β,β-caroten-4-one
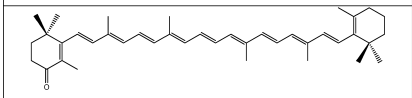	Echinenone β,β-caroten-4-one
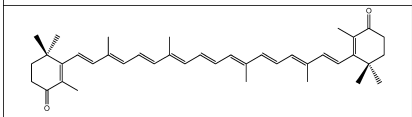	Canthaxanthin β,β-carotene-4,4'-dione
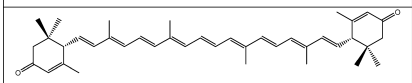	3,3'-Dioxo-ε-carotene (6*S*,6'*S*)-ε,ε-carotene-3,3'-dione
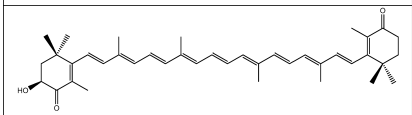	Adonirubin (3*R*)-3-hydroxy-β,β-carotene-4,4'-dione
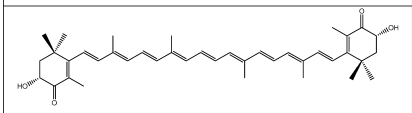	Astaxanthin (3*R*,3'*R*)-3,3'-dihydroxy-β,β-carotene-4,4'-dione
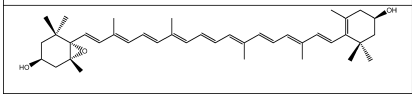	Antheraxanthin (3*R*,5*R*,6*S*,3'*R*)-5,6-epoxy-5,6-dihydro-β,β-carotene-3,3'-diol
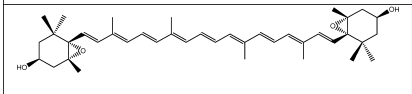	Violaxanthin (3*S*,5*R*,6*S*,3'*S*,5'*R*,6'*S*)-5,6,5',6'-diepoxy-5,6,5',6'-tetrahydro-β,β-carotene-3,3'-diol

Figure 2. Structure and nomenclature of the xanthophylls investigated in this work.

IE_{exp} (6.32 eV) and phytoene the highest (7.00 eV), in agreement with the literature.[21] For a fixed number of CDB, cyclization at one end does not influence IE, whereas cyclisation at both ends is moderately detrimental to ionization (lycopene: 6.32 eV, γ-carotene: 6.33 eV, β-carotene: 6.41 eV), possibly because of slight distortions shifting endocyclic CDB out of the plane of the linear polyene chain.

Oxygenation (N_{CDB} set constant) generally leads to an increase of IE, as evidenced by the following examples:

1. Hydroxylation: γ-carotene (6.33 eV) < rubixanthin (6.56 eV), α-carotene (6.35 eV) < zeinoxanthin (6.52 eV) < lutein (6.57 eV). An exception: β-carotene (6.41 eV) > β-cryptoxanthin (6.34 eV).
2. Presence of carbonyl groups: β-carotene (6.45 eV) < echinenone (6.53 eV) < canthaxanthin (6.75 eV), ε-carotene (6.48 eV) < dioxo-ε-carotene (6.89 eV), β-cryptoxanthin (6.34 eV) < adonirubin (6.86).
3. Epoxidation: zeaxanthin (6.43 eV) < antheraxanthin and violaxanthin (6.53 and 6.57 eV, resp.).

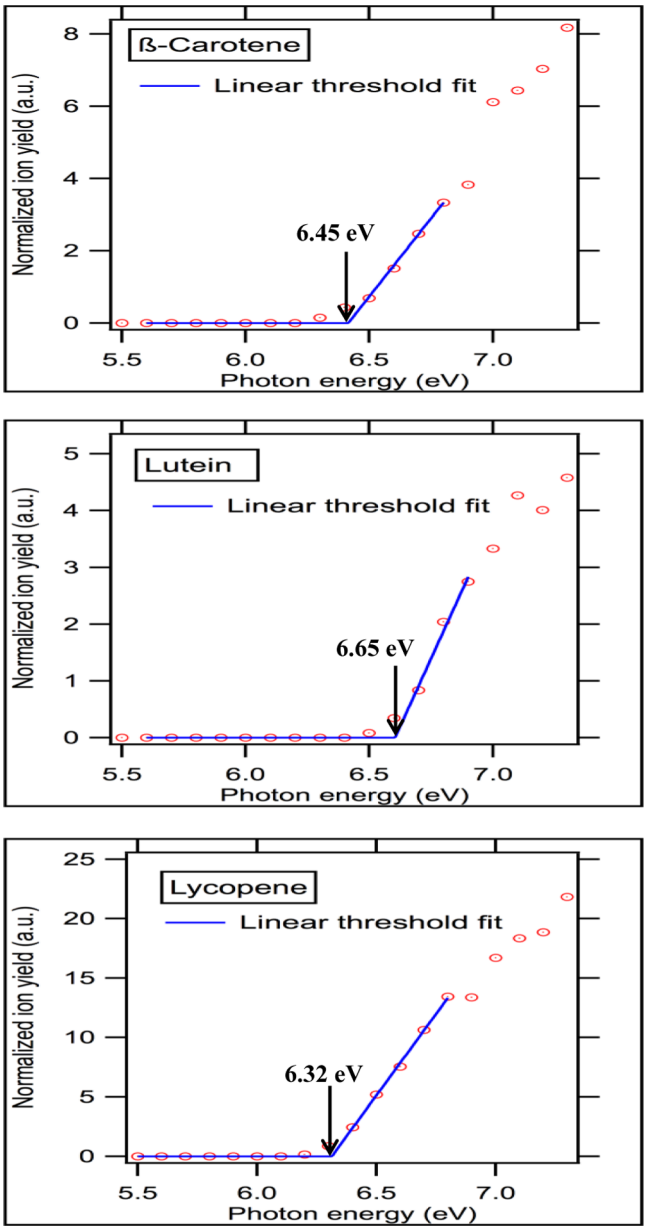

Figure 3. Photoionization yields for β-carotene, lutein, and lycopene, normalized to the flux (red symbols). Linear fitting to data (blue line) yields the ionization threshold.

Figure 4 shows a selection of the highest occupied π molecular orbitals (HOMO) obtained by ab initio calculations. The terminal ends of the carotenoids investigated are not involved in the HOMO. Both IE_{cal} and IE_{exp} are higher than the calculated values in the literature.[9,11]

Antioxidant Activity. Inhibiting the peroxidation of dietary polyunsaturated fatty acids (PUFAs) by natural antioxidants is important for food preservation during processing and storage

DOI: 10.1021/acs.jpcb.8b03447
J. Phys. Chem. B 2018, 122, 5860−5869

Table 1. Structures, IC_{50} (μM), IE_{exp}, and IE_{cal} (eV) of the Carotenoids Investigated

	terminus	CDB	OH	C=O	IC_{50}*	IE_{exp}	IE_{cal}	$IE_{exp} - IE_{cal}$
lycopene	1ψ,1ψ	11			1.98 ± 0.14^{g,h,i}	6.32 ± 0.13	6.61	−0.29
neurosporene	1ψ,1ψ	9			2.19 ± 0.06^{g,h}	6.35 ± 0.10	6.66	−0.31
ζ-carotene	1ψ,1ψ	7			3.14 ± 0.21^{d}	6.46 ± 0.10	6.74	−0.28
phytofluene	1ψ,1ψ	5			5.91 ± 0.56^{b}	6.63 ± 0.10	6.96	−0.30
phytoene	1ψ,1ψ	3			13.63 ± 1.33^{a}	7.00 ± 0.10	7.26	−0.26
β-carotene	2β	11			2.08 ± 0. 27^{g,h}	6.41 ± 0.10	6.44	−0.03
α-carotene	1β,1ε	10			2.53 ± 0.23^{e,f,g,h}	6.35 ± 0.10	6.46	−0.11
ε-carotene	2ε	9			3.07 ± 0.36^{d,e}	6.48 ± 0.10	6.48	0.00
γ-carotene	1β,1ψ	11			1.28 ± 0.14^{j}	6.33 ± 0.02	6.64	−0.31
δ-carotene	1ε,1ψ	10			1.93 ± 0.10^{g,h,i}	6.33 ± 0.10	6.66	−0.33
β-zeacarotene	1β,1ψ	9			2.28 ± 0.25^{g,h,i}	6.51 ± 0.20	6.73	−0.22
rubixanthin	1β,1ψ	11	1		1.44 ± 0.12^{i,j}	6.56 ± 0.10	6.67	−0.11
anhydrolutein III	2β	12	1		1.85 ± 0.16^{h,i}	6.48 ± 0.10	6.46	0.02
β-cryptoxanthin	2β	11	1		2.26 ± 0.08^{g,h}	6.34 ± 0.10	6.46	−0.12
zeaxanthin	2β	11	2		2.39 ± 0.10^{e,f,g,h}	6.43 ± 0.10	6.46	−0.03
zeinoxanthin	1β,1ε	10	1		2.59 ± 0.12^{d,e,f,g}	6.52 ± 0.10	6.46	0.06
lutein	1β,1ε	10	2		2.67 ± 0.11^{e,f,g,h}	6.57 ± 0.10	6.48	0.09
tunaxanthin E	2ε	9	2		3.13 ± 0.15^{d,e,f}	nd	6.52	
echinenone	2β	11	0	1	2.41 ± 0.08^{e,f,g,h}	6.53 ± 0.10	6.59	−0.06
canthaxanthin	2β	11	0	2	3.02 ± 0.27^{d,e,f}	6.75 ± 0.10	6.70	0.05
dioxo-ε-carotene	2ε	9	0	2	4.67 ± 0.24^{c}	6.89 ± 0.15	6.74	0.15
adonirubin	2β	11	1	2	3.24 ± 0.29^{f,g,h}	6.86 ± 0.15	6.71	0.15
adonixanthin	2β	11	2	1	2.31 ± 0.19^{j,k}	6.75 ± 0.25	6.57	0.18
astaxanthin	2β	11	2	2	2.63 ± 0.20^{d,e,f,g}	6.67 ± 0.10	6.73	−0.06
antheraxanthin	1β	10	2	1**	2.54 ± 0.28^{e,f,g,h}	6.53 ± 0.10	6.49	0.04
violaxanthin		9	2	2**	3.95 ± 0.14^{c}	6.57 ± 0.10	6.61	−0.04

*Means with no letters in common differ significantly (ANOVA post hoc SNK, $p < 0.05$). **Epoxy (instead of oxo).

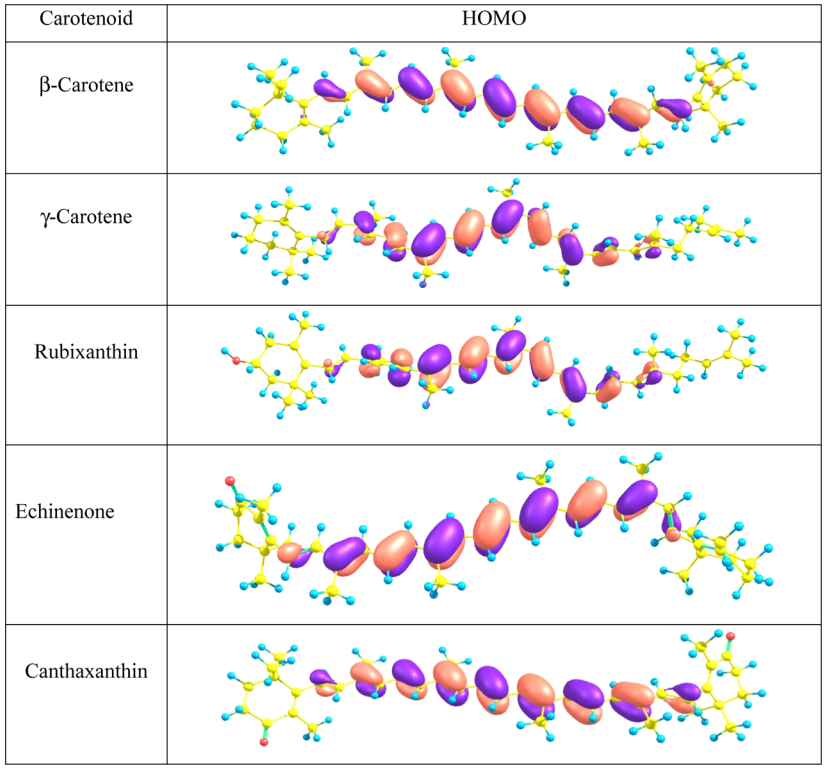

Figure 4. HOMO pictures of a selection of carotenoids obtained by ab initio calculations.

but may also be significant after ingestion of food. Indeed, the stomach is a site where PUFAs (noted LH to outline a labile bis-allylic H-atom, inevitably contaminated by traces of lipid hydroperoxides LOOH), O_2, and dietary iron can combine under vigorous stirring in acidic conditions, thus creating conditions for further lipid peroxidation.[22] This form of

DOI: 10.1021/acs.jpcb.8b03447
J. Phys. Chem. B 2018, 122, 5860−5869

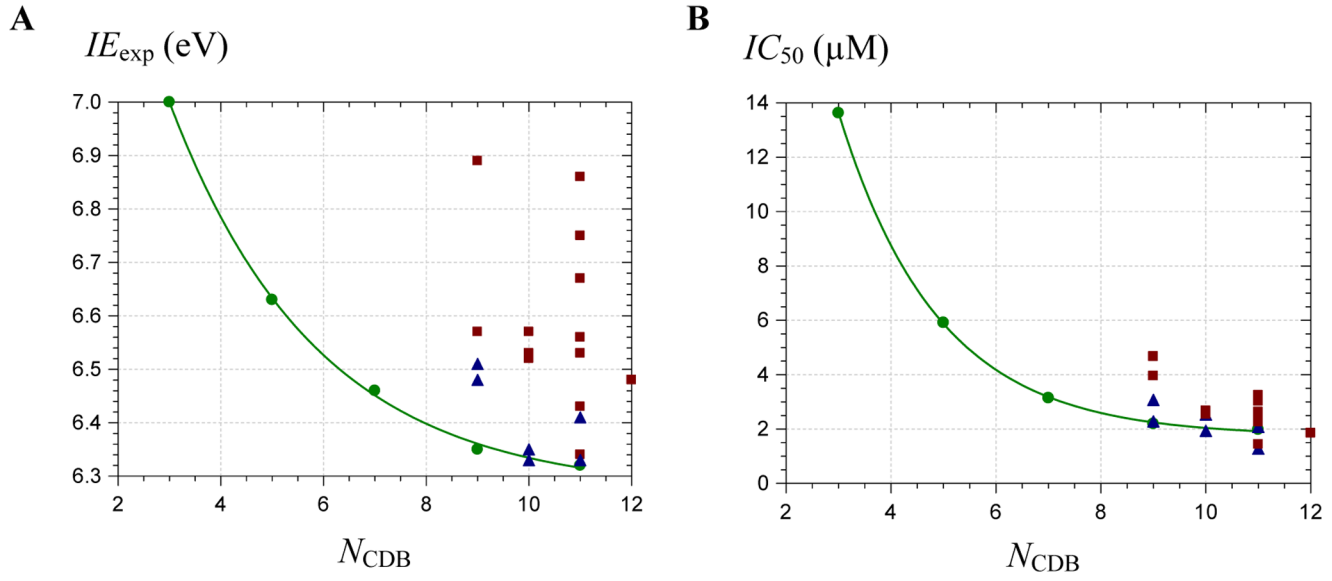

Figure 5. (A) Plot of the experimental ionization energy as a function of the number of conjugated double bonds. The exponential curve fitting (solid line) applies to the five acyclic carotenes only. $IE_{exp} = A \exp(-BN_{CDB}) + C$, A = 2.1 (±0.1), B = 0.35 (±0.02), C = 6.27 (±0.02), r = 0.9996. (B) Plot of the IC_{50} of heme-induced lipid peroxidation as a function of the number of conjugated double bonds. The exponential curve fitting (solid line) applies to the five acyclic carotenes only. $IC_{50} = A \exp(-BN_{CDB}) + C$, A = 58.1 (±1.8), B = 0.53 (±0.01), C = 1.74 (±0.06), r = 0.99995. The green circle solid: acyclic carotenes, the blue triangle up solid: cyclic carotenes, the red box solid: xanthophylls.

postprandial oxidative stress and its inhibition by dietary antioxidants, such as phenolic compounds and carotenoids, can be easily modeled.[18,23] In this work, oxidation is efficiently initiated by metmyoglobin ($MbFe^{III}$), one of the main forms of dietary iron (red meat). Using this model, we were able to demonstrate that hydrophilic and lipophilic antioxidants display distinct inhibition mechanisms[16] and discriminate lycopene and its derivatives ((*Z*)-isomers, oxygenated cleavage products).[17]

The IC_{50} values of the carotenoids investigated lie between 1.28 μM for γ-carotene (best inhibitor, 11 CDB) and 13.63 μM for phytoene (weakest inhibitor, three CDB) (Table 1). For all carotenes, the antioxidant activity increases with the number of CDB, although the differences are not significant with most carotenes having 9−11 CDB. For a fixed number of CDB, bicyclic carotenoids are systematically less potent than monocyclic ones. By contrast, monocyclic γ-carotene is more potent than acyclic lycopene.

In the literature, lycopene (acyclic) was found to be a better scavenger of the bulky ABTS radical cation than γ-carotene (one β-ionone ring) and β-carotene (two β-ionone rings).[24]

With xanthophylls, no significant correlation could be found between the number of CDB and IC_{50}. The trend we observed that hydroxylation and more significantly the presence of keto groups (β-carotene > echinenone > canthaxanthin, ε-carotene > dioxo-ε-carotene) lower the antioxidant activity is consistent with the literature.[24−26] Xanthophylls bearing two strongly electron-withdrawing keto groups conjugated with the polyene chain (canthaxanthin vs β-carotene, adonirubin vs β-cryptoxanthin, and astaxanthin vs zeaxanthin) actually have lower radical-scavenging activities than analogs with the same number of CDB. More surprisingly, 3,3′-dioxo-ε-carotene is less potent than ε-carotene, although its two keto groups are unconjugated with the polyene chain.

5,6-Mono and bis-epoxidation of zeaxanthin, leading to antheraxanthin and violaxanthin, lower the antioxidant activity and this probably reflects the decrease in the number of CDB.

DISCUSSION

The general correlation between the number of CDB and the antioxidant properties of carotenoids has been well established using various models.[7,8,10,24] However, for a fixed number of CDB, correlations with other structural characteristics are more difficult to outline. In particular, oxygenation in the carotenoid structure means introducing, not only more or less electron-withdrawing groups tending to increase IE, but also more polar heads with a higher affinity for the aqueous phase. While the former effect is expected to weaken the antioxidant activity, the latter could act in the opposite direction if the positioning of the carotenoid within the micelles is closer to that of the lipid peroxyl radicals, which themselves bear a terminal polar head (the carboxyl/carboxylate group).

Within the class of acyclic carotenes, the number of conjugated double bonds has a drastic influence on IE and an exponential decrease is observed when N_{CDB} increases (Figure 5A). Extrapolation to an infinite number of CDB yields a theoretical IE of 6.27 eV. Taking this curve as a reference, it can be seen that cyclic carotenes obey this general trend, although a slight destabilization is observed with β-carotene, ε-carotene, and β-zeacarotene (0.10−0.15 eV above the curve). By contrast, most xanthophylls lie well out of the curve, suggesting that any oxygenated substituent raises IE and thus weakens the electron-donating capacity. The most spectacular deviations concern the following group: adonirubin > dioxo-ε-carotene > adonixanthin, canthaxanthin > astaxanthin (0.55−0.36 eV above the curve). It is especially striking that adonirubin and dioxo-ε-carotene, despite their 11 and 9 CDB, are barely better electron donors than phytoene (3 CDB) and anyway weaker than phytofluene (5 CDB). Interestingly, although adonirubin must be severely deactivated by the strong electron-withdrawing mesomeric effect of both keto groups conjugated with the polyene moiety, this is not so with dioxo-ε-carotene, as each terminal enone moiety is separated from the polyene by a saturated C-atom. However, both xanthophylls display near

DOI: 10.1021/acs.jpcb.8b03447
J. Phys. Chem. B 2018, 122, 5860−5869

Scheme 2. Inhibition of Linoleic Acid Peroxidation by γ-Carotene (R = H) and Rubixanthin (R = OH) (N_{CDB} = 11)[a]

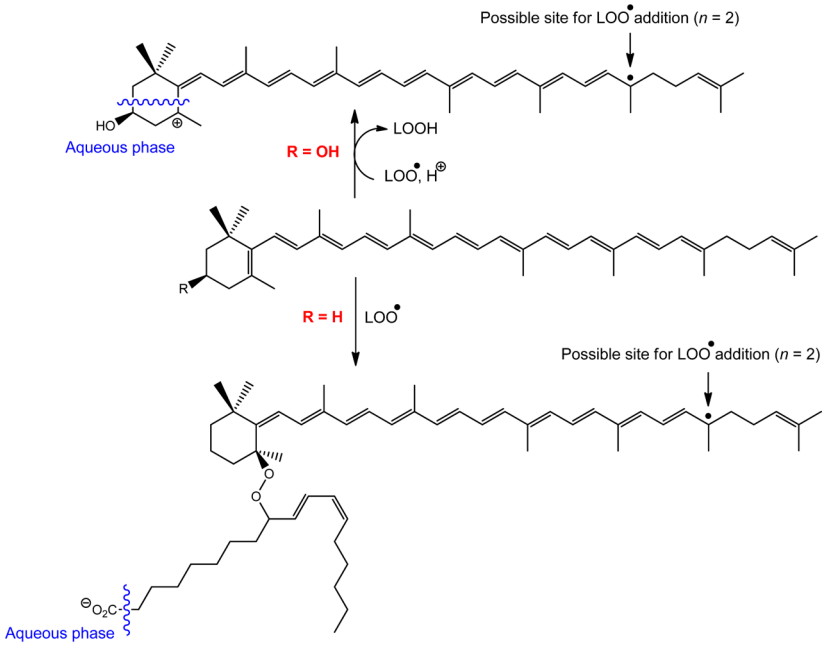

[a]Possible mechanisms involving electron transfer and radical addition. Scavenging of the first LOO• radical (n = 1) may be followed by addition of a second one (n = 2) and subsequent reactions with the shorter polyene moiety (N_{CDB} = 10) (n > 2).

equal IE (ΔIE = 0.03 eV), whether experimental or calculated values are considered. It seems that the electron-withdrawing inductive effect of both enone moieties strongly destabilizes the radical cation of dioxo-ε-carotene.

The method can be repeated to analyze the dependence of IC_{50} on the number of CDB (Figure 5B). Again, an exponential decrease is observed when N_{CDB} increases. Extrapolation to an infinite number of CDB yields a theoretical IC_{50} of 1.74 μM. Except rubixanthin (0.47 μM below correlation), which interestingly is the sole monocyclic xanthophyll investigated, all xanthophylls are poorer antioxidants (higher IC_{50} above reference curve built from the five acyclic carotenes) than anticipated from the number of their CDB. This is especially true for dioxo-ε-carotene, violaxanthin, adonirubin, and canthaxanthin (IC_{50} 2.44, 1.72, 1.33, and 1.11 μM above correlation, resp.). Among cyclic carotenes, the differences are less pronounced but more contrasted with ε-carotene lying 0.84 μM above correlation and γ-carotene (one of the three monocyclic carotenes investigated) lying 0.63 μM below (more antioxidant than anticipated).

Being lipophilic, carotenes are expected to lie at the core of the lipid phase and exert their antioxidant activity by addition of LOO• to the ends of the polyene chain, so as to ensure maximal electron delocalization in the neutral radical adduct (Scheme 2). By contrast, electron transfer could take place following interaction between the two reagents all along the polyene chain. However, electron transfer should be unfavorable with carotenes as the radical cation would be produced in a nonpolar environment. The proposal of radical scavenging operating by radical addition to the carotenes' polyene ends is consistent with the slightly lower antioxidant activity observed when both ends are cyclized, thereby bringing steric hindrance.

Having an amphiphilic character due to one or two more polar end(s), xanthophylls might inhibit lipid peroxidation by a combination of electron transfer and radical addition (Scheme 2). Indeed, shifting the xanthophylls' ends toward the aqueous phase to ensure solvation of the polar groups could also stabilize the corresponding radical cation. Anyway, both mechanisms are favored by a HOMO of high energy (low IE, high nucleophilicity).

It must be kept in mind that IC_{50} is a global parameter assessing the antioxidant activity. It must combine kinetic and stoichiometric factors, i.e. not only the rate constant of radical scavenging but also the number of radicals scavenged per equivalent of antioxidant. To outline this point, a quantitative kinetic analysis was launched with a selection of carotenoids: on the one hand, γ-carotene and rubixanthin, on the other hand, β-carotene, echinenone, and canthaxanthin, to respectively investigate the influence of OH and keto groups for a fixed number of CDB. The kinetic model with the corresponding parameters is depicted in Scheme 1. The early stage of linoleic acid (LH) peroxidation is relatively simple as it mainly corresponds to the accumulation of hydroperoxides (LOOH). However, these primary products are rather unstable and could be partially decomposed, not only by reaction with the heme initiator, but also by unidentified metal traces (e.g., from the phosphate buffer and/or the surfactant) contaminating the medium. Over a few hours, experiments with freshly prepared solutions were found highly reproducible. However, control experiments (uninhibited peroxidation) repeated day-after-day (before investigating any new antioxidant) showed significant discrepancies and could not be correctly analyzed without assuming low contaminating metal concentrations (c_M) involved in LOOH decomposition (second-order rate constant k_M). With this correction (c_M and k_M being additional adjustable parameters), perfect curve fittings were obtained, yielding reliable sets of values for the oxidizability (r_{ox}) and the rate constant of LOOH decomposition by metmyoglobin (k_{i1}) (Table 2). Regarding the inhibited peroxidation, the curve fittings of the A (234 nm) vs time curves using the r_{ox} and k_{i1} values previously determined were also fully satisfactory (Figure 6) and gave reproducible values for the additional adjustable

DOI: 10.1021/acs.jpcb.8b03447
J. Phys. Chem. B 2018, 122, 5860−5869

Table 2. Kinetic Analysis of Metmyoglobin-Induced Peroxidation of Linoleic Acid

Uninhibited Peroxidation (Control Experiments)				
carotenoid	r_{ox} ($M^{-1/2}$ $s^{-1/2}$)	k_{i1} ($\times 10^3$) (M^{-1} s^{-1})	k_M (M^{-1} s^{-1})	C_M (μM)
γ-carotene (N = 4)	1.70 (±0.12)	11.0 (±0.6)	489 (±131)	11.8 (±4.8)
rubixanthin (N = 2)	1.53 (±0.01)	8.2 (±0.6)	429 (±89)	9.4 (±0.5)
β-carotene (N = 4)	2.09 (±0.02)	15.0 (±0.3)	547 (±21)	23.7 (±0.9)
echinenone (N = 4)	1.87 (±0.01)	13.3 (±0.6)	473 (±19)	15.1 (±1.0)
canthaxanthin (N = 5)	1.96 (±0.09)	14.3 (±0.7)	643 (±41)	11.6 (±2.9)
Inhibited Peroxidation				
carotenoid, C_0 (μM)	AE	n	nAE	C_d (nM)
γ-carotene, 1 (N = 4)	64 (±6)	6.2 (±0.2)	396.8	148 (±15)
2 (N = 4)	65 (±4)	3.6 (±0.1)	234	176 (±14)
3 (N = 4)	68 (±4)	2.9 (±0.1)	197.2	164 (±2)
4 (N = 2)	68 (±1)	2.4 (±0.1)	163.2	158 (±1)
5 (N = 4)	69 (±5)	2.1 (±0.1)	144.9	151 (±2)
rubixanthin, 1 (N = 4)	73 (±5)	4.9 (±0.2)	357.7	157 (±7)
2 (N = 4)	78 (±8)	3.2 (±0.2)	249.6	178 (±10)
3 (N = 4)	73 (±1)	2.4 (±0.1)	175.2	192 (±3)
4 (N = 3)	65 (±2)	2.2 (±0.1)	143	177 (±2)
5 (N = 4)	69 (±4)	1.9 (±0.1)	131.1	176 (±2)
β-carotene, 1 (N = 4)	85 (±1)	5.0 (±0.1)	425	176 (±10)
2 (N = 4)	78 (±2)	3.2 (±0.1)	249.6	179 (±4)
3 (N = 4)	75 (±1)	2.6 (±0.1)	195	169 (±3)
4 (N = 4)	72 (±2)	2.3 (±0.1)	165.6	151 (±6)
5 (N = 4)	70 (±1)	2.1 (±0.1)	147	139 (±1)
echinenone, 1 (N = 4)	71 (±2)	4.3 (±0.1)	305.3	182 (±9)
2 (N = 4)	73 (±11)	2.6 (±0.1)	189.8	196 (±3)
3 (N = 4)	71 (±2)	2.2 (±0.1)	156.2	209 (±3)
4 (N = 4)	71 (±1)	1.8 (±0.1)	127.8	201 (±2)
5 (N = 4)	70 (±1)	1.6 (±0.1)	112	182 (±1)
canthaxanthin, 1 (N = 4)	77 (±7)	4.1 (±0.3)	315.7	102 (±25)
2 (N = 5)	69 (±1)	2.6 (±0.1)	179.4	156 (±6)
3 (N = 6)	60 (±3)	2.2 (±0.1)	132	170 (±6)
4 (N = 5)	56 (±1)	1.9 (±0.1)	106.4	174 (±4)
5 (N = 5)	53 (±1)	1.7 (±0.1)	90.1	171 (±5)

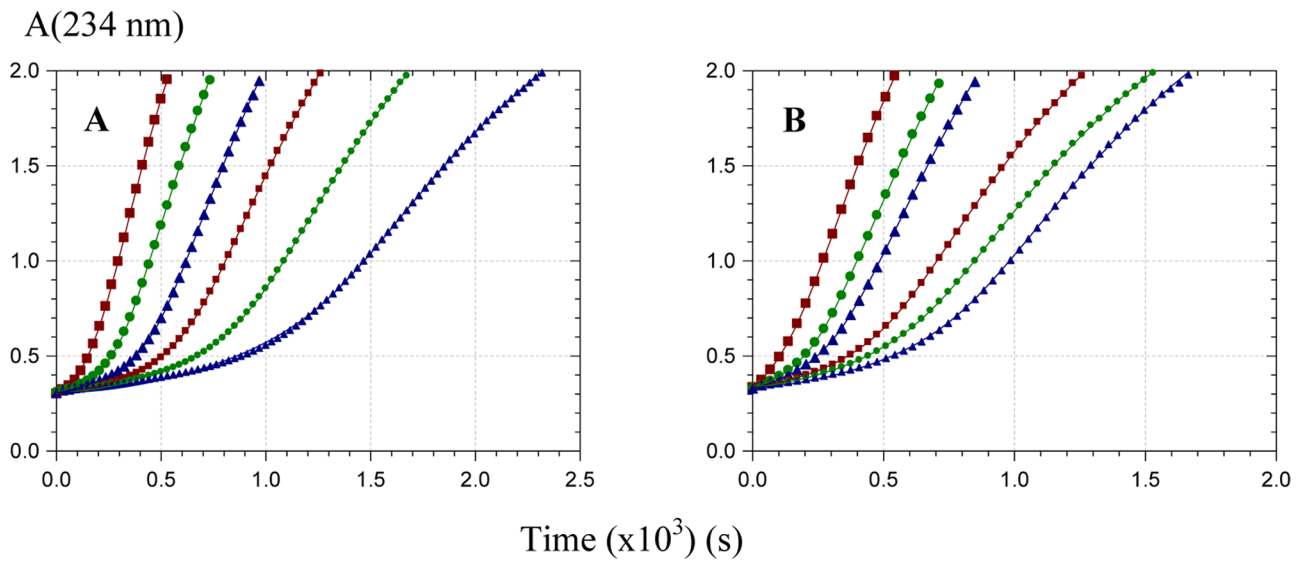

Figure 6. Inhibition of the metmyoglobin-induced peroxidation of linoleic acid in Tween 20 micelles, pH 5.8, 37 °C, antioxidant concentration = 0–5 μM. (A) β-Carotene, (B) echinenone.

parameters pertaining to the antioxidant: the antioxidant efficiency at inhibiting propagation (AE = k(Car + LOO$^\bullet$)/k(LH + LOO$^\bullet$) = k_{ip}/k_p) and its stoichiometry (n) (Table 2). Antioxidants capable of scavenging more than one radical equivalent (n > 1) can be modeled as combinations of n theoretical antioxidant subunits, each reacting with LOO$^\bullet$ with

DOI: 10.1021/acs.jpcb.8b03447
J. Phys. Chem. B 2018, 122, 5860–5869

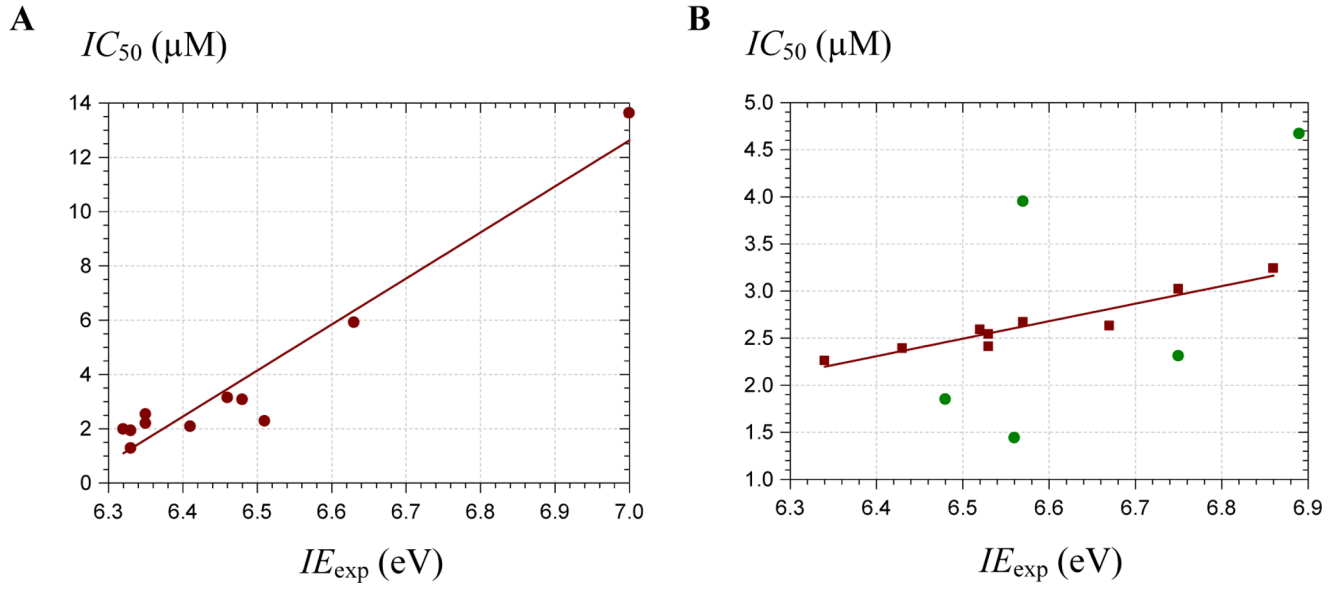

Figure 7. Plot of the IC_{50} of heme-induced lipid peroxidation as a function of the experimental ionization energy. (A) Carotenes (11 compounds), r = 0.96. (B) Xanthophylls (r = 0.60), the red box solid: selection (nine compounds), r = 0.95, the green circle solid: anhydrolutein III, rubixanthin, adonixanthin (below correlation), violaxanthin, and dioxo-ε-carotene (above correlation).

the same mean rate constant k_{ip}. Thus, the nk_{ip} product is a better estimate of the rate constant for the initial scavenging step involving the intact carotenoid (transfer of the first electron and/or addition of the first $LOO^{\bullet}$). Hence, the nAE product is also reported in Table 2.

Finally, as inhibited peroxidation is typically monitored over longer periods of time than uninhibited peroxidation, heme degradation becomes significant and must be accounted for by parameter C_d, which is homogenous to a concentration and expresses the competitive fates of hypervalent heme: cleavage of LOOH to generate $LOO^{\bullet}$ vs heme decomposition.

The optimized parameters permit to emphasize the following point: as long as carotenoids have a long conjugated polyene moiety (N_{CDB} = 9 or 11 in the series investigated), they are potent inhibitors of lipid peroxidation with only weak differences in their stoichiometry and rate constant of radical scavenging. For each carotenoid, the stoichiometry and the nAE product decay when the antioxidant concentration is increased. This drift suggests that carotenoids tend to associate in micelles and that the aggregates thus formed are less efficient than individual carotenoid molecules at scavenging the lipid peroxyl radicals.

If electron transfer makes a higher contribution to radical scavenging by xanthophylls due to their more polar environment, the distribution of oxidation products should be different from that obtained with analogous carotenes. With xanthophylls, the formation of more polar oxidation products, displaced to the aqueous phase and thus no longer active for radical scavenging, could explain the slightly lower stoichiometric factors. On the other hand, even polar products released into the aqueous phase could participate in the inhibition by reducing the hypervalent form of metmyoglobin involved in the initiation step (Scheme 1). For instance, both apo-14′-lycopenoic acid (a short-chain cleavage product and potential metabolite of lycopene, N_{CDB} = 6) and crocin (a water-soluble carotenoid from saffron, N_{CDB} = 7) were shown to reduce ferrylmyoglobin ($MbFe^{IV}$=O) produced by reacting $MbFe^{III}$ with H_2O_2.[17,27] Anyway, the typical stoichiometry range of 2−5 points to a minimal scavenging of two $LOO^{\bullet}$ equivalents (Scheme 2), which is consistent with theoretical predictions[20] and experimental analyses of carotenoid−radical adducts.[28]

CONCLUSIONS

In this work, the coupling of an atmospheric pressure photoionization source with a synchrotron radiation beam line in the vacuum UV allowed performing tunable photoionization mass spectrometry with carotenoids, which are difficult to vaporize by classical methods.

Carotenes and xanthophylls with at least nine CDB are efficient inhibitors of heme-induced lipid peroxidation in mildly acidic conditions, the carotenes lycopene and γ-carotene emerging as the best ones, followed by rubixanthin, a hydroxy-carotenoid.

The ionization energy is a reliable predictor of the antioxidant activity of carotenes, as shown by the good correlation between IE and IC_{50} (r = 0.96, 11 compounds, Figure 7A). This is much less so with xanthophylls and a good correlation (r = 0.95) is only obtained with a selection of 9 compounds out of the total of 15 (Figure 7B). For instance, rubixanthin is a much better antioxidant than anticipated from its IE, whereas the reverse is true for violaxanthin and dioxo-ε-carotene. Part of these discrepancies could be rooted in the specific fate of these xanthophylls in the course of the radical-scavenging process, i.e. in the residual activity of some of their oxidation products.

ASSOCIATED CONTENT

Supporting Information

The Supporting Information is available free of charge on the ACS Publications website at DOI: 10.1021/acs.jpcb.8b03447.

Heme-induced lipid peroxidation; the mathematical treatment used for the analysis of the conjugated diene concentration vs time curves is provided (PDF)

DOI: 10.1021/acs.jpcb.8b03447
J. Phys. Chem. B 2018, 122, 5860−5869

AUTHOR INFORMATION

Corresponding Author

*E-mail: olivier.dangles@univ-avignon.fr.

ORCID

Alexandre Giuliani: 0000-0003-1710-4933
Denis Duflot: 0000-0002-8307-5344
Olivier Dangles: 0000-0002-9501-0644

Notes

The authors declare no competing financial interest.

ACKNOWLEDGMENTS

This work was funded by the French National Institute for Agricultural Research (INRA) through its ANS program aimed at stimulating innovative research.

REFERENCES

(1) Namitha, K. K.; Negi, P. S. Chemistry and biotechnology of carotenoids. *Crit. Rev. Food Sci. Nutr.* **2010**, *50*, 728−760.

(2) Desmarchelier, C.; Borel, P. Overview of carotenoid bioavailability determinants: From dietary factors to host genetic variations. *Trends Food Sci. Technol.* **2017**, *69*, 270−280.

(3) Fernández-García, E.; Carvajal-Lerida, I.; Jaren-Galan, M.; Garrido-Fernandez, J.; Perez-Galvez, A.; Hornero-Mendez, D. Carotenoids bioavailability from foods: From plant pigments to efficient biological activities. *Food Res. Int.* **2012**, *46*, 438−450.

(4) Bernstein, P. S.; Li, B.; Vachali, P. P.; Gorusupudi, A.; Shyam, R.; Henriksen, B. S.; Nolan, J. M. Lutein, zeaxanthin, and meso-zeaxanthin: The basic and clinical science underlying carotenoid-based nutritional interventions against ocular disease. *Prog. Retinal Eye Res.* **2016**, *50*, 34−66.

(5) Kaulmann, A.; Bohn, T. Carotenoids, inflammation, and oxidative stress—implications of cellular signaling pathways and relation to chronic disease prevention. *Nutr. Res.* **2014**, *34*, 907−929.

(6) Skibsted, L. H. Carotenoids in antioxidant networks. Colorants or radical scavengers. *J. Agric. Food Chem.* **2012**, *60*, 2409−2417.

(7) Müller, L.; Fröhlich, K.; Böhm, V. Comparative antioxidant activities of carotenoids measured by ferric reducing antioxidant power (FRAP), ABTS bleaching assay (TEAC), DPPH assay and peroxyl radical scavenging assay. *Food Chem.* **2011**, *129*, 139−148.

(8) Bauerfeind, J.; Hintze, V.; Kschonsek, J.; Killenberg, M.; Böhm, V. Use of photochemiluminescence for the determination of antioxidant activities of carotenoids and antioxidant capacities of selected tomato products. *J. Agric. Food Chem.* **2014**, *62*, 7452−7459.

(9) Galano, A. Relative antioxidant efficiency of a large series of carotenoids in terms of one electron transfer reactions. *J. Phys. Chem. B* **2007**, *111*, 12898−12908.

(10) El-Agamey, A.; Lowe, G. M.; McGarvey, D. J.; Mortensen, A.; Phillip, D. M.; Truscott, T. G.; Young, A. J. Carotenoid radical chemistry and antioxidant/pro-oxidant properties. *Arch. Biochem. Biophys.* **2004**, *430*, 37−48.

(11) Martínez, A.; Rodriguez-Girones, M. A.; Barbosa, A.; Costas, M. Donator acceptor map for carotenoids, melatonin and vitamins. *J. Phys. Chem. A* **2008**, *112*, 9037−9042.

(12) Dougherty, D.; Younathan, E. S.; Voll, R.; Abdulnur, S.; McGlynn, S. P. Photoelectron-spectroscopy of some biological molecules. *J. Electron Spectrosc. Relat. Phenom.* **1978**, *13*, 379−393.

(13) Giuliani, A.; Giorgetta, J. L.; Ricaud, J. P.; Jamme, F.; Rouam, V.; Wien, F.; Laprevote, O.; Refregiers, M. Atmospheric pressure photoionization using tunable VUV synchrotron radiation. *Nucl. Instrum. Methods Phys. Res., Sect. B* **2012**, *279*, 114−117.

(14) Giuliani, A.; Jamme, F.; Rouam, V.; Wien, F.; Giorgetta, J.-L.; Lagarde, B.; Chubar, O.; Bac, S.; Yao, I.; Rey, S.; et al. DISCO: a low-energy multipurpose beamline at synchrotron SOLEIL. *J. Synchrotron Radiat.* **2009**, *16*, 835−841.

(15) Giuliani, A.; Yao, I.; Lagarde, B.; Rey, S.; Duval, J.-P.; Rommeluere, P.; Jamme, F.; Rouam, V.; Wein, F.; De Oliveira, C.; et al. A differential pumping system to deliver windowless VUV photons at atmospheric pressure. *J. Synchrotron Radiat.* **2011**, *18*, 546−549.

(16) Vulcain, E.; Goupy, P.; Caris-Veyrat, C.; Dangles, O. Inhibition of the metmyoglobin-induced peroxidation of linoleic acid by dietary antioxidants: Action in the aqueous vs lipid phase. *Free Radic. Res.* **2005**, *39*, 547−563.

(17) Goupy, P.; Reynaud, E.; Dangles, O.; Caris-Veyrat, C. Antioxidant activity of (all-E)-lycopene and synthetic apo-lycopenoids in a chemical model of oxidative stress in the gastro-intestinal tract. *New J. Chem.* **2012**, *36*, 575−587.

(18) Sy, C.; Caris-Veyrat, C.; Dufour, C.; Boutaleb, M.; Borel, P.; Dangles, O. Inhibition of iron-induced lipid peroxidation by newly identified bacterial carotenoids in model gastric conditions. Comparison with common carotenoids. *Food Funct.* **2013**, *4*, 698−712.

(19) Szabo, A.; Ostlund, N. S. *Modern Quantum Chemistry: Introduction to Advanced Electronic Structure Theory*; Courier Corporation: New York, 1996.

(20) Martínez, A.; Vargas, R.; Galano, A. Theoretical study of the chemical fate of adducts formed through free radical addition reactions to carotenoids. *Theor. Chem. Acc.* **2010**, *127*, 595−603.

(21) Martínez, A.; Stinco, C. M.; Melendez-Martinez, A. J. Free radical scavenging properties of phytofluene and phytoene isomers as compared to lycopene: a combined experimental and theoretical study. *J. Phys. Chem. B* **2014**, *118*, 9819−9825.

(22) Gobert, M.; Remond, D.; Loonis, M.; Buffiere, C.; Sante-Lhoutellier, V.; Dufour, C. Fruits, vegetables and their polyphenols protect dietary lipids from oxidation during gastric digestion. *Food Funct.* **2014**, *5*, 2166−2174.

(23) Achat, S.; Rakotomanomana, N.; Madani, K.; Dangles, O. Antioxidant activity of olive phenols and other dietary phenols in model gastric conditions: scavenging of the free radical DPPH and inhibition of the haem-induced peroxidation of linoleic acid. *Food Chem.* **2016**, *213*, 135−142.

(24) Miller, N. J.; Sampson, J.; Candeias, L. P.; Bramley, P. M.; Rice-Evans, C. A. Antioxidant activities of carotenes and xanthophylls. *FEBS Lett.* **1996**, *384*, 240−242.

(25) Mortensen, A.; Skibsted, L. H. Importance of carotenoid structure in radical-scavenging reactions. *J. Agric. Food Chem.* **1997**, *45*, 2970−2977.

(26) Rodrigues, E.; Mariutti, L. R. B.; Chiste, R. C.; Mercadante, A. Z. Development of a novel micro-assay for evaluation of peroxyl radical scavenger capacity: Application to carotenoids and structure-activity relationship. *Food Chem.* **2012**, *135*, 2103−2111.

(27) Jørgensen, L. V.; Andersen, H. J.; Skibsted, L. H. Kinetics of reduction of hypervalent iron in myoglobin by crocin in aqueous solution. *Free Radical Res.* **1997**, *27*, 73−87.

(28) Liebler, D. C.; McClure, T. D. Antioxidant reactions of β-carotene: identification of carotenoid-radical adducts. *Chem. Res. Toxicol.* **1996**, *9*, 8−11.

DOI: 10.1021/acs.jpcb.8b03447
J. Phys. Chem. B 2018, 122, 5860−5869